

ORIGINAL RESEARCH

Cardiac Gene Therapy With Phosphodiesterase 2A Limits Remodeling and Arrhythmias in Mouse Models of Heart Failure

Rima Kamel, PhD^{*}; Aurélia Bourcier , PhD^{*}; Jean Piero Margaria, PhD^{*}; Valentin Jin, MSc; Audrey Varin , MSc; Agnès Hivonnait , MSc; Françoise Mercier-Nomé , MSc; Delphine Mika , PhD; Alessandra Ghigo , PhD; Flavien Charpentier , PhD; Vincent Algalarrondo , MD, PhD; Emilio Hirsch , PhD; Rodolphe Fischmeister , PhD; Grégoire Vandecasteele , PhD; Jérôme Leroy , PhD

BACKGROUND: PDE2 (phosphodiesterase 2) is upregulated in human heart failure. Cardiac PDE2-transgenic mice are protected against contractile dysfunction and arrhythmias in heart failure but whether an acute elevation of PDE2 could be of therapeutic value remains elusive. This hypothesis was tested using cardiac PDE2 gene transfer in preclinical models of heart failure.

METHODS AND RESULTS: C57BL/6 male mice were injected with serotype 9 adeno-associated viruses encoding for PDE2A. This led to a ~10-fold rise of PDE2A protein levels that affected neither cardiac structure nor function in healthy mice. Two weeks after inoculation with serotype 9 adeno-associated viruses, mice were implanted with minipumps delivering either NaCl, isoproterenol (60 mg/kg per day), or isoproterenol and phenylephrine (30 mg/kg per day each) for 2 weeks. In mice injected with serotype 9 adeno-associated viruses encoding for LUC (luciferase), isoproterenol or isoproterenol+phenylephrine infusion induced left ventricular hypertrophy, decreased ejection fraction unveiled by echocardiography, and promoted fibrosis and apoptosis assessed by Masson's trichrome and Tunel, respectively. Furthermore, inotropic responses to isoproterenol of ventricular cardiomyocytes isolated from isoproterenol+phenylephrine-LUC mice loaded with 1 μ M Fura-2AM and stimulated at 1 Hz to record calcium transients and sarcomere shortening were dampened. Spontaneous calcium waves at the cellular level were promoted as well as ventricular arrhythmias evoked in vivo by catheter-mediated ventricular pacing after isoproterenol (1.5 mg/kg) and atropine (1 mg/kg) injection. However, increased PDE2A blunted these adverse outcomes evoked by sympathomimetic amines.

CONCLUSIONS: Cardiac gene therapy with PDE2A limits left ventricle remodeling, dysfunction, and arrhythmias evoked by catecholamines, providing evidence that increasing PDE2A activity acutely could prevent progression toward heart failure.

Key Words: arrhythmia ■ cAMP-phosphodiesterase ■ catecholamines ■ excitation-contraction coupling ■ gene therapy ■ heart failure

The “fight-or-flight” response involves a discharge of norepinephrine by the sympathetic nervous system, causing the secretion of catecholamines

by the adrenal medulla that act on cardiomyocytes via the β -adrenergic receptor (β -AR)/AC (adenylyl cyclase)/cAMP/PKA (protein kinase A) axis to stimulate

Correspondence to: Jérôme Leroy, PhD and Rodolphe Fischmeister, PhD, INSERM UMR-S 1180, Université Paris-Saclay, Faculté de Pharmacie, Bât. Henri Moissan, 17, avenue des sciences, 91400 Orsay, France. Email: jerome.leroy@universite-paris-saclay.fr; rodolphe.fischmeister@inserm.fr

^{*}R. Kamel, A. Bourcier, and J. P. Margaria contributed equally.

Preprint posted on BioRxiv April 20, 2023. <https://doi.org/10.1101/2023.04.17.537274>.

This article was sent to Julie K. Freed, MD, PhD, Associate Editor, for review by expert referees, editorial decision, and final disposition.

Supplemental Material is available at <https://www.ahajournals.org/doi/suppl/10.1161/JAHA.124.037343>

For Sources of Funding and Disclosures, see page 14.

© 2025 The Author(s). Published on behalf of the American Heart Association, Inc., by Wiley. This is an open access article under the terms of the [Creative Commons Attribution-NonCommercial-NoDerivs](#) License, which permits use and distribution in any medium, provided the original work is properly cited, the use is non-commercial and no modifications or adaptations are made.

JAHA is available at: www.ahajournals.org/journal/jaha

RESEARCH PERSPECTIVE

What Is New?

- PDE2A (phosphodiesterase 2A) expression is increased in heart failure and cardiac PDE2-transgenic mice are protected against contractile dysfunction and arrhythmia in heart failure; however, it is unknown whether an acute increase in PDE2A activity can prevent maladaptive remodeling and exert antiarrhythmic effects.
- We show that increased PDE2A expression using AAV9 encoding for this enzyme limits left ventricular hypertrophy, fibrosis, and dysfunction induced by sympathomimetic amines and improves defective β -adrenergic receptor inotropic effects of isolated cardiomyocytes.
- Increasing PDE2A exerts antiarrhythmic effects both at the cellular level and in vivo and is more efficient than increasing PDE4B to prevent ventricular tachycardias.

What Question Should Be Addressed Next?

- These data suggest that an acute increase in PDE2A activity is of therapeutic potential in heart failure but warrants further testing in larger animal models and clinical studies.

Nonstandard Abbreviations and Acronyms

AAV9	serotype 9 adeno-associated viruses
AC	adenylyl cyclase
CaT	calcium transients
ECC	excitation-contraction coupling
LUC	luciferase
PDE	phosphodiesterase
PDE2	phosphodiesterase 2
SS	sarcomere shortening
TL	tibia length
VM	ventricular myocyte
β-AR	β -adrenergic receptor

cardiac rhythm (chronotropy), contractile force (inotropy), and relaxation (lusitropy).¹ PKA phosphorylates many of the proteins critically involved in the excitation-contraction coupling (ECC). These include the small G protein Rad to stimulate the L-type Ca^{2+} channels,² the ryanodine receptor 2 to increase its open probability, the phospholamban to relieve its inhibitory effect on the sarco/endoplasmic reticulum Ca^{2+} -ATPase, and contractile proteins, such as troponin I and myosin

binding protein C.¹ Although this acute β -AR activation is favorable allowing the adaptation of the cardiac output to increased body's metabolic demand during a stress or an effort, a chronic overactivation of the sympathetic nervous system is deleterious. In heart failure (HF), the decreased cardiac function leads to a chronic catecholamine elevation³ that elicits maladaptive remodeling comprising cardiac hypertrophy, cardiomyocyte death, and cardiac fibrosis and promotes arrhythmias thus aggravating pump dysfunction. The excessive β -AR stimulation is central in this propelled vicious circle as attested by the beneficial effects of β -AR antagonists that are the first-line therapy to treat chronic HF with reduced ejection fraction.^{4,5} However, despite an enhancement in survival rates by the use of β -blockers,⁵⁻⁷ the mortality of patients with HF 5 years after diagnosis mainly due to pump failure or ventricular arrhythmias remains unacceptably high at ~50%.⁸ Furthermore, in many patients, intolerance does not allow titration to an effective dosage.⁹ There is thus a need for new therapeutic approaches to treat HF.

Intracellular cAMP levels produced upon β -AR stimulation are counterbalanced by the degradation of the cyclic nucleotide by enzymes called PDEs (phosphodiesterases) that not only terminate the activation of cAMP effectors but also compartmentalize this second messenger in discrete subcellular compartments.¹⁰ Among the 6 PDE families expressed in cardiomyocytes to degrade cAMP, PDE2 has been recently identified as a therapeutic target to treat HF. PDE2 was shown to inhibit cardiac L-type Ca^{2+} channel activity in various species, including humans¹¹ and to control ECC even though it exhibits rather low protein expression and its inhibition has little effect on cAMP hydrolytic activity in healthy cardiomyocytes.¹²⁻¹⁴ In contrast to PDE3 and PDE4, the 2 main enzymes degrading cAMP in the heart, expression and activities of which are generally decreased in pathological hypertrophy and HF,¹⁵⁻¹⁷ PDE2 is increased in HF to blunt β -AR/cAMP signals suggesting a protective mechanism against increased circulating catecholamines.¹⁸ Accordingly, transgenic mice with constitutive cardiac overexpression of PDE2 exhibit improved cardiac function and are protected against catecholamine-induced arrhythmias after ischemic injury.¹⁹ Moreover, PDE2 hydrolytic activity is stimulated by 10- to 30-fold by cGMP via binding to the regulatory N-terminal GAF-B domain²⁰ making PDE2 a unique integrator of cAMP/cGMP signals.^{14,21,22} Interestingly, a recent study unveiled that the antiarrhythmic effects of C-type natriuretic peptide occur via PDE2 stimulation, attenuating spontaneous Ca^{2+} events, limiting CaMKII (calcium/calmodulin-stimulated protein kinase II) activation and decreasing the late Na^{+} current promoted by a β -AR stimulation.²³ However, the cardioprotective effects of increased PDE2 activity are a matter of debate because conflicting results

reported that PDE2 upregulation is prohypertrophic.²² Furthermore, its inhibition was found to antagonize cardiomyocyte growth²² and to protect against apoptotic cell death by promoting mitochondrial elongation²⁴ and PDE2 blockade with BAY60-7550 hindered cardiac maladaptive remodeling by enhancing nitric oxide/guanylyl cyclase/cGMP signaling.²⁵

In an attempt to further delineate the impact of PDE2 upregulation on cardiac function and its putative beneficial effects in HF, we performed gene therapy with adeno-associated viruses serotype 9 (AAV9) allowing substantial cardiac overexpression of PDE2A3.²⁶ This strategy allows expression from a definite time point rather than constitutive cardiac expression as previously employed.¹⁹ With this strategy, we demonstrated in vivo that PDE2 overexpression protects the heart upon a chronic exposure to sympathomimetic amines (phenylephrine or isoproterenol), by reducing remodeling and left ventricular (LV) dysfunction. Strikingly, increased cardiac PDE2A expression prevents ventricular arrhythmias upon stress and this correlates with improved ECC at the level of single cardiomyocytes.

METHODS

Data Availability Statement

The data that support the findings of this study are available from the corresponding authors upon reasonable request.

Ethical Approval and Animals

All procedures were carried out at the animal facility and at the laboratory INSERM UMR-S 1180 of the faculty of Pharmacy of the Paris-Saclay University, according to institutional regulations and the local guide for the use and care of laboratory animals. All experiments involving animals were conducted in agreement with the European Community guiding principles in the welfare and use of animals (2010/63/UE) and the French decree no. 2013-118 on the protection of animals used for scientific purposes. The protocol was approved by the local ethics committee (CREEA Ile-de-France Sud) and by the French Ministry of Higher Education and Research (17852-2015051 112 125554 v4). In this study, 8-week-old male C57BL/6 mice obtained from Janvier Labs were used. Before the start of all experimental protocols, 7 days of acclimatization were respected. Mice used in this study were housed in ventilated cages (GM550 Greenline, Tecniplast France) with enrichment and were exposed to 12-hour light/dark nonreverse cycles (light from 7 AM to 7 PM) in a thermostatically and humidity-controlled room (21–22°C, 40%–50% humidity) at our institute's animal facility (ANIMEX IPSIT, approval number B92-019-01). Mice had free access to a standard diet (A03 Safe for breeding, A04 Safe during experimental protocols) and water. Mice

were never isolated and were distributed into experimental groups randomly. The animals were monitored daily to evaluate the physical appearance (observation every day) and weight (measurement 3 times/week). When a weight loss of 10% to 20% compared with the initial weight was observed, access to food was facilitated. None of the animals included in the experimental protocols reached end points such as a weight loss >20%.

Reagents

Isoproterenol, phenylephrine, and atropine were purchased from Sigma-Aldrich (St. Louis, MO). Bay60-7550 was purchased from Cayman chemical (Ann Arbor, MI).

AAV9-LUC/PDE Vectors Production, Purification, Characterization, and Injection

AAV9-PDE2A holds a PDE2A3 expression cassette flanked by 2 AAV2 inverted terminal repeats. The expression sequence is pseudotyped with an AAV9 capsid. The cassette contains a human cytomegalovirus (CMV) promoter, a β -globin intron, a FLAG tag fused in 5' of the complete murine PDE2A3 coding sequence (NCBI: NM_001008548.4), and a human growth hormone polyadenylation signal. AAV9-PDE2A was produced in AAV-293T cells (Stratagene #240073, San Diego, CA) with the 3-plasmid method and the calcium-chloride transfection. The virus was purified by cesium-chloride gradient. A real-time polymerase chain reaction on the CMV promoter was used to determine viral particles titers. An expression cassette encoding firefly LUC (luciferaseLUC) was used for control condition. A CMV promoter controlling LUC expression was packaged into AAV9 capsids and purified on cesium-chloride gradient to yield AAV9-LUC virus. AAV9-LUC or AAV9-PDE2A were injected via the tail vein at 10^{12} viral particles/mouse. AAV9-CMV is the empty control vector used to produce AAV9-PDE2A containing solely the CMV promoter without any open reading frame sequence. The AAV9-PDE4B has been previously described.¹⁵

Transthoracic Echocardiography

Transthoracic 2-dimensional-guided M-mode echocardiography of mice was performed using an echocardiograph with an ML6 linear probe of 15MHz (Vivid E9, General Electric Healthcare, Chicago, IL) under 1% to 2% isoflurane gas and 0.4 to 0.8L/min oxygen anesthesia. For isoflurane induction, mice were placed for approximately 2 minutes in an isolation chamber filled with isoflurane (5% in 100% oxygen) at a flow rate of 0.5 to 1L/min. Body temperature was maintained at 37°C by the use of a thermally controlled heating pad (Harvard Apparatus). Measurements from animals with heart frequencies <400bpm were discarded. LV cavity and wall thickness dimensions during

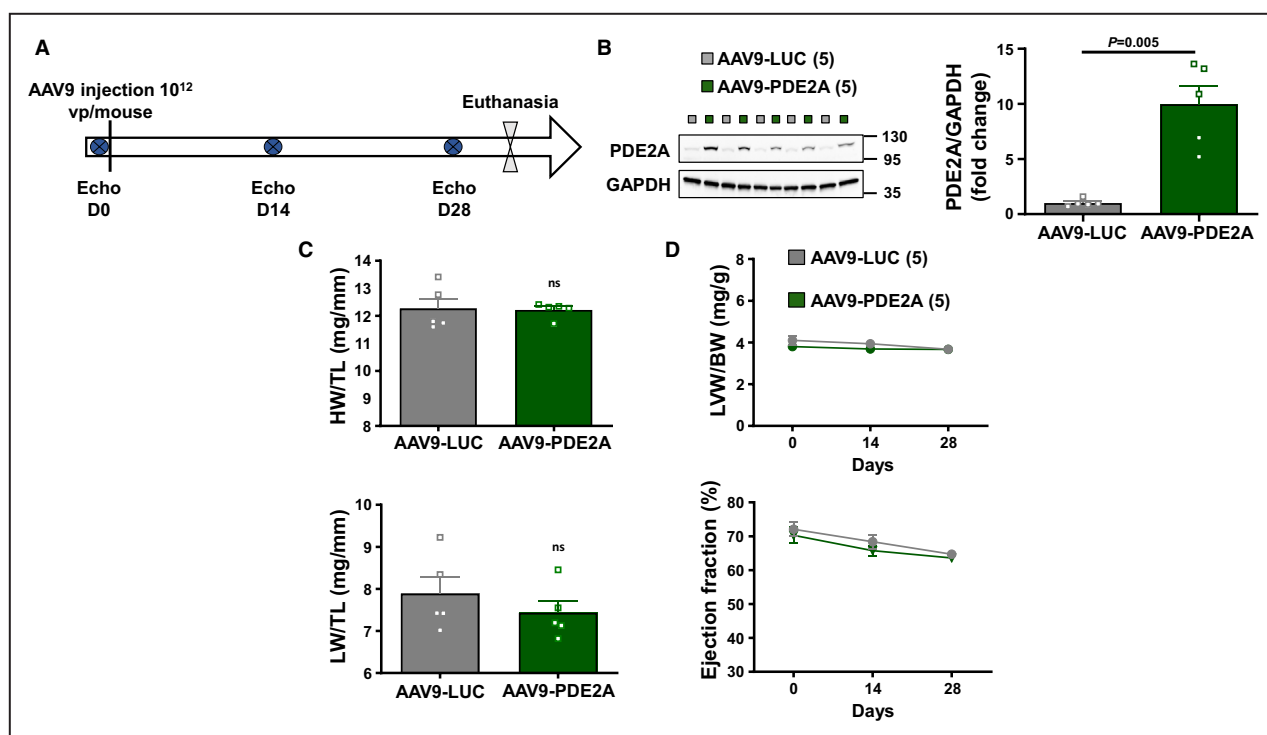


Figure 1. PDE2A overexpression by AAV9 does not alter cardiac function or morphological parameters.

A, Schematic representation of the experimental protocol. Mice were injected in the tail vein with 10^{12} viral particles of serotype 9 adeno-associated viruses encoding for Luciferase or phosphodiesterase 2A3. Twenty-eight days later, mice were euthanized. Cardiac function was assessed throughout the protocol by echocardiography before, then 2 and 4 weeks after the injection of the recombinant viruses. **B**, Left panel shows representative blots of PDE2A and GAPDH, the bar graph represents the ratios of PDE2A over GAPDH quantified, expressed as mean \pm SEM of fold change in cardiac tissues from AAV9-LUC and AAV9-PDE2A mice. **C**, Heart weight and lung weight over tibia length ratios expressed as mean \pm SEM. **D**, Time course of ejection fraction and the ratio of calculated left ventricular weight over body weight in AAV9-LUC and AAV9-PDE2A mice. Number of mice is indicated in the brackets. Statistical significance is indicated by the *P* value determined using Welch's *t*-test (**B**) Mann–Whitney (HW/TL) and unpaired Student's *t* test (LW/TL) (**C**), 2-way ANOVA followed by Tukey's test (**D**). AAV9 indicates serotype 9 adeno-associated viruses; BW, body weight; HW, heart weight; LUC, luciferase; LVW, left ventricular weight; LW, lung weight; PDE2A, phosphodiesterase 2A; and TL, tibia length.

systole and diastole were determined using 2 parasternal axes: short and long. The LV weight was calculated according to the Penn formula while assuming a spherical LV geometry and validated for the mouse heart ($LV\ mass = 1.04 \times [(LV\ internal\ diameter + interventricular\ septum\ thickness + posterior\ wall\ thickness)^3 - (LV\ internal\ diameter\ in\ diastole)^3]$), where 1.04 is the specific density in g/cm³ of muscle. Analysis was performed for the echocardiographic images using the EchoPac software (General Electric Healthcare). For each of the 2 axes and the measured parameters, 3 measurements on 3 different sections were averaged. Analysis of the echocardiography data was blinded to the mice population.

Sympathomimetic Amines Infusion Models

Schematic representations of the experimental protocols used to treat animals are depicted in [Figures 1A](#),

[2A](#), and [3A](#). Briefly, a first echocardiography to assess cardiac function before AAV9 injections was performed. Two weeks after, a second echocardiography was realized and sympathomimetic amines administered via osmotic minipumps (2002, Alzet, Cupertino, CA) surgically implanted subcutaneously in the back of the animals as previously described.¹⁵ This allowed treatment of the animals for 14 days with either isoproterenol (60 mg/kg per day), isoproterenol+phenylephrine (30 mg/kg per day each), or vehicle (0.9% NaCl). An intermediate echocardiography at day 21 was performed on animals treated with isoproterenol+phenylephrine, a last one at day 28 before euthanasia after minipump removal to avoid interference on the cardiac function of remaining sympathomimetic treatment ([Figure 3A](#)). Cardiac function was followed at day 28 when the minipump was removed and for 2 additional weeks for the isoproterenol model by echocardiography performed at days 35 and 42.

Morphological and Histological Analysis

For euthanasia, mice were anesthetized by an intraperitoneal injection of pentobarbital (Doléthal, 100mg/kg). Afterwards, hearts were rapidly excised and remaining blood was washed out in cold Ca^{2+} -free PBS solution (155.2mmol/L NaCl, 1.06mmol/L KH_2PO_4 and 2.9mmol/L NaH_2PO_4). Hearts and lungs were weighed and tibia length (TL) was measured. For histology, a transversal slice of 3 to 4 mm width was cut in the middle of the heart and rapidly fixed in 4% paraformaldehyde. The rest of ventricular tissue was frozen in liquid nitrogen and stored at -80°C until use.

Histological staining was performed using a standard protocol. After fixation of the hearts for 24 hours in 4% paraformaldehyde, they were paraffin embedded and transversely sectioned. Sections (5 or 7 μm) were deparaffinized. Afterwards, samples were subjected to Heat-Induced Epitope Retrieval in a 10mmol/L citrate buffer, pH=6. A Masson's trichrome stain kit (Microm, Brignais, France) was used to assess cardiac fibrosis. To quantify apoptotic myocytes in the heart, autofluorescence was quenched by treating paraffin-embedded sections with PBS/BSA (5%) for 2 hours before performing TUNEL staining (Roche, Basel,

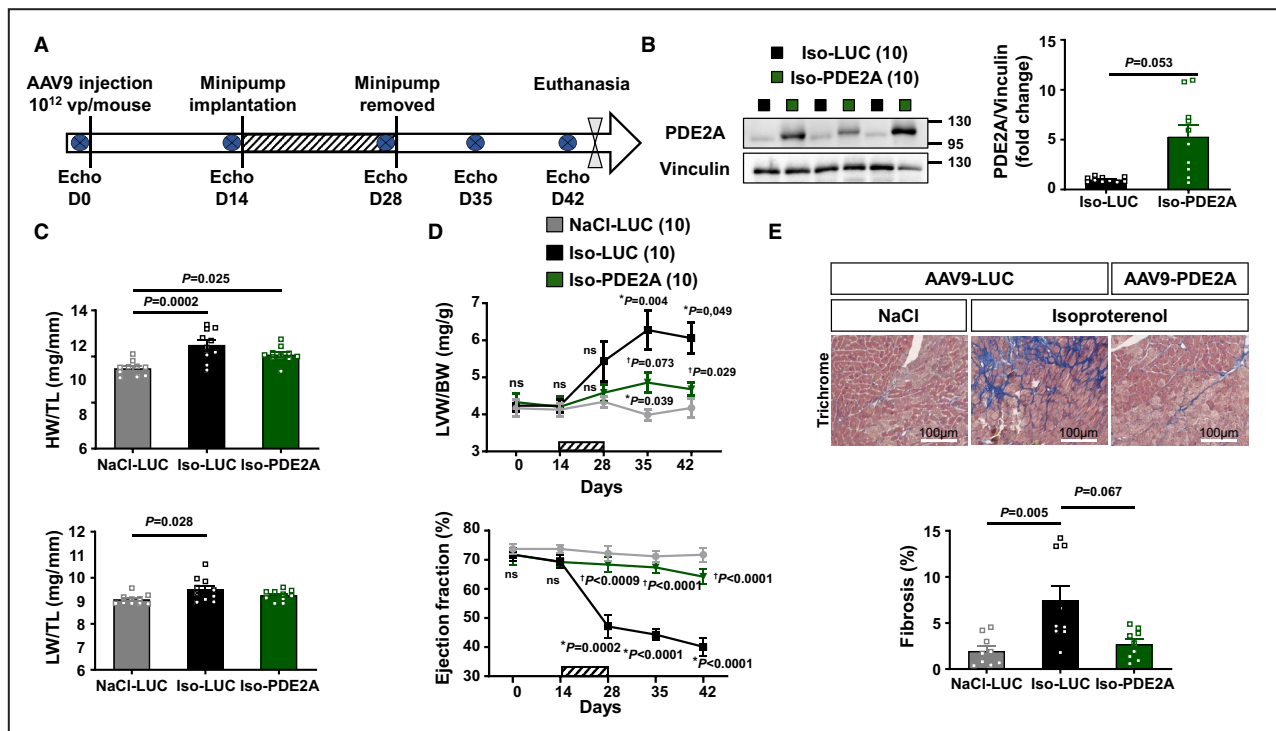


Figure 2. Gene therapy with PDE2A prevents cardiac remodeling and dysfunction induced by chronic isoproterenol infusion.

A, Schematic representation of the experimental protocol. Mice were injected in the tail vein with 10^{12} viral particles of a serotype 9 adeno-associated viruses encoding for luciferase or phosphodiesterase 2A3. Fourteen days later, mice injected with AAV9-LUC were implanted subcutaneously with osmotic pumps diffusing either NaCl (NaCl-LUC) or isoproterenol at 60 mg/kg per day (isoproterenol-LUC) and animals injected with AAV9-PDE2A were implanted with pumps delivering isoproterenol at 60 mg/kg per day (isoproterenol-PDE2A). Treatment duration was 14 days (hatched bars). Minipumps were then removed and mice were kept for 2 additional weeks before euthanasia. Cardiac function was evaluated by serial echocardiography before injection of the virus as well as at 14, 28, 35, and 42 days. **B**, Left panel shows representative blots of PDE2A and vinculin. PDE2A protein expression in heart tissues extracts measured by Western blot and the bar graph represents the ratios of PDE2A over vinculin quantified expressed as mean \pm SEM in NaCl-LUC, isoproterenol-LUC and isoproterenol-PDE2A groups. **C**, Heart weight and lung weight over tibia length ratio expressed as mean \pm SEM. **D**, Time course of the normalized ratio of calculated left ventricular weight over body weight and normalized ejection fraction in NaCl-LUC, isoproterenol-LUC and isoproterenol-PDE2A mice. Number of mice is indicated in the brackets. **E**, Panel on the left, representative images of Masson's trichrome staining (scale bar 100 μm), bar graph on the left represents quantifications of interstitial fibrosis as mean \pm SEM in NaCl-LUC (n=9), isoproterenol-LUC (n=9), and isoproterenol+PDE2A (n=9) groups. Statistical significance is indicated by the P value (* vs NaCl-LUC and † vs isoproterenol-LUC) determined using Welch's t test (**B**), Kruskal-Wallis followed by a Dunn's test (**C** panel bottom and **E**), 2-way ANOVA followed by a Tukey's test (**D**), 1-way ANOVA followed by a Tukey's test (**C** panel top). AAV9 indicates serotype 9 adeno-associated viruses; BW, body weight; HW, heart weight; Iso-LUC, isoproterenol-luciferase; Iso-PDE2A, isoproterenol-phosphodiesterase 2A; LUC, luciferase; LVW, left ventricular weight; LW, lung weight; PDE2A, phosphodiesterase 2A; and TL, tibia length.

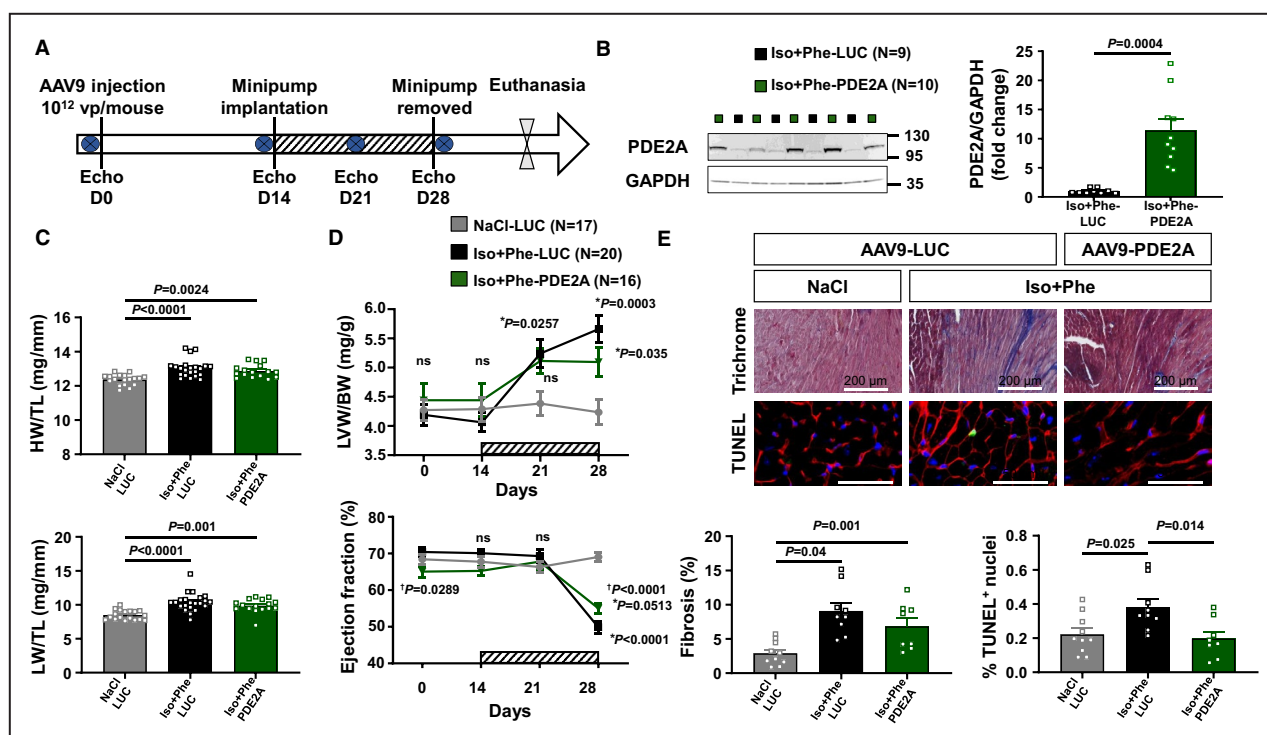


Figure 3. PDE2A overexpression limits maladaptive remodeling and cardiac dysfunction induced by chronic isoproterenol and phenylephrine infusion.

A, Schematic representation of the experimental protocol. Mice were injected with 10^{12} viral particles of serotype 9 adeno-associated viruses encoding for Luciferase or phosphodiesterase 2A3. Fourteen days later, mice were implanted with osmotic minipumps diffusing either NaCl (NaCl-LUC) or isoproterenol+phenylephrine at 30 mg/kg per day each (isoproterenol+phenylephrine-LUC and isoproterenol+phenylephrine-PDE2A). Minipumps were removed 2 weeks later and mice were euthanized. Cardiac function was assessed throughout the protocol using echocardiography before the injection of the virus and at 2, 3, 4, and 6 weeks. **B**, Representative blots of PDE2A and GAPDH on the left panel are shown and the bar graph represents ratios of PDE2A over GAPDH quantifications expressed as mean \pm SEM in a subset of the animals treated with NaCl-LUC, isoproterenol+phenylephrine-LUC, and isoproterenol+phenylephrine-PDE2A. **C**, Heart weight and lung weight over tibia length ratios expressed as mean \pm SEM. **D**, Time course of the normalized ratios of calculated left ventricular weight (over body weight) and normalized ejection fraction in NaCl-LUC, isoproterenol+phenylephrine-LUC, and isoproterenol+phenylephrine-PDE2A mice. Number of mice is indicated in the brackets. **E**, Top panel shows representative images of Masson's trichrome staining (scale bar 200 μ m), the middle panel depicts representative images of terminal deoxynucleotidyl transferase dUTP nick end labeling (TUNEL) assay (scale bar 100 μ m) detecting apoptotic nuclei in green costained with the glycolocalyx marker wheat germ agglutinin in red and nuclei in blue colored with Hoechst. Bar graphs representing mean \pm SEM quantifications of interstitial fibrosis and apoptotic nuclei in NaCl-LUC (10), isoproterenol+phenylephrine-LUC (9) and isoproterenol+phenylephrine-PDE2A (9) mice are depicted. Statistical significance indicated by the *P* value (* vs NaCl-LUC and † vs isoproterenol+phenylephrine-LUC) was determined using Welch's *t* test (**B**), Kruskal–Wallis followed by a Dunn's test (**C**), 2-way ANOVA followed by a Tukey's test (**D**), Welch's 1-way ANOVA followed by a Dunnett's test (**E**). AAV9 indicates serotype 9 adeno-associated viruses; BW, body weight; HW, heart weight; Iso-Phe-LUC, isoproterenol-phenylephrine-luciferase; Iso-Phe-PDE2A, isoproterenol-phenylephrine-phosphodiesterase 2A; LUC, luciferase; LVW, left ventricular weight; LW, lung weight; ns, not significant; PDE2A, phosphodiesterase 2A; and TL, tibia length.

Switzerland) according to the manufacturer's protocol and using Proteinase K treatment. Sections were counterstained with Alexa Fluor 594-conjugated wheat germ agglutinin (WGA, Invitrogen, Carlsbad, CA) at 10 μ g/mL for 1 hour at room temperature to visualize cell membranes. Slides were scanned by the digital slide scanner NanoZoomer 2.0-RS (Hamamatsu, Japan), which allowed an overall view of the samples and analyzed blinded to the mice population. Images were digitally captured from the scan slides using the NDP.view2 software (Hamamatsu, Japan).

ECG Recording and Intracardiac Recording and Pacing

The criteria used to measure RR, PR, QRS, and QT intervals on recorded ECG have been described elsewhere.²⁷ The QT interval was corrected for heart rate with the Bazett formula adapted to mouse sinus rate, that is, $QT_c = QT / (RR/100)^{1/2}$ with QT and RR, expressed in ms.²⁸ Mice were anesthetized with an intraperitoneal injection of etomidate of 28 mg/kg (Hypnomidate 2 mg/mL, Janssen-Cilag, Issy les Moulineaux, France) before

and after intracardiac and surface ECG recording and pacing. The extremity of a 2F octopolar catheter 1.5 French (Cordis Webster) was placed in the right ventricle through the right internal jugular vein, using intracardiac electrograms as a guide for catheter positioning in the right ventricle. Surface ECG (lead I) and intracardiac electrograms were recorded on a computer through an analog-digital converter (IOX 1.585, Emka Technologies, Paris, France) for monitoring and later analysis (ECG-Auto v3.3.0.5, Emka Technologies, Paris, France). Intracardiac electrograms were filtered between 0.5 and 500 Hz. Pacing was performed with a digital stimulator (DS8000, World Precision Instruments, Sarasota, FL). The standard pacing protocols were used to determine the ventricular effective refractory periods and to induce ventricular arrhythmias were developed as follows: Determination of stimulation threshold, which corresponds to the minimal energy provoking a ventricular depolarization, was done with 1-ms-long pulses with increasing intensity. Afterwards, stimulations were conducted at intensities 1.5 times the excitation threshold. Ventricular effective refractory periods were assessed at baseline by using the programmed electrical stimulation method. Extrastimuli were delivered following trains of 20 pulses at a cycle length of 70 milliseconds followed by 1, 2, and then 3 extrastimuli. The extrastimulus coupling interval was initially set at 70 milliseconds and then reduced by 2 milliseconds at each cycle until ventricular refractoriness was reached. The inducibility of ventricular arrhythmias was assessed in baseline conditions and 3 minutes after intraperitoneal injection of isoproterenol 1.5 mg/kg and atropine 1 mg/kg. Ventricular tachycardias were defined as the occurrence of at least 4 consecutive QRS complexes with a morphology different from that seen with a normal sinus rhythm, after last stimulated beat.

Isolation of Mouse Cardiomyocytes

Mice were anesthetized by intraperitoneal injection of Doléthal (100 mg/kg). The heart was quickly removed and placed into a cold Ca^{2+} -free Tyrode's solution containing 113 mmol/L NaCl, 4.7 mmol/L KCl, 1.2 mmol/L $\text{MgSO}_4 \cdot 7\text{H}_2\text{O}$, 0.6 mmol/L KH_2PO_4 , 0.6 mmol/L NaH_2PO_4 , 1.6 mmol/L NaHCO_3 , 10 mmol/L HEPES, 30 mmol/L taurine, 20 mmol/L glucose, and 17.03 $\mu\text{mol/L}$ insulin adjusted to pH 7.4. The ascending aorta was cannulated, and the heart was perfused at constant pressure (≈ 798 mmHg, flow rate = 26 mL/min) with oxygenated Ca^{2+} -free Tyrode's solution at 37 °C for approximately 4 minutes using retrograde Langendorff perfusion. Subsequently, the heart was perfused with Ca^{2+} -free Tyrode's solution containing Liberase research grade (Roche Diagnostics, Basel, Switzerland) for 10 minutes at 37 °C for enzymatic dissociation. Afterwards, the heart was removed and placed in a dish containing a Tyrode's

solution supplemented with 0.2 mmol/L CaCl_2 and 5 mg/mL BSA (Sigma-Aldrich, St. Louis, MO). Atria were discarded and ventricles were cut into small pieces and triturated gently with a pipette to disperse the myocytes. Ventricular myocytes were filtered on gauze and allowed to sediment by gravity for approximately 7 minutes. The supernatant was removed, and cells were suspended in Tyrode's solution supplemented with 0.5 mmol/L CaCl_2 and 5 mg/mL BSA. Sedimentation was repeated and cells were finally suspended in a Tyrode's solution with 1 mmol/L CaCl_2 . For Ionoptix experiments, freshly isolated ventricular myocytes were plated for 45 minutes at a density of 10^4 cells per dish in 35-mm culture dishes coated with laminin (10 $\mu\text{g/mL}$) and stored in a cell incubator at 37 °C, 5% CO_2 until use up to 4 hours.

Calcium Transients and Sarcomere Shortening Measurements

Isolated cardiomyocytes were loaded with 1 $\mu\text{mol/L}$ fura-2 AM (Invitrogen, Carlsbad, CA) at room temperature for 15 minutes and then washed for 15 additional minutes with an external Ringer solution containing (in mM): NaCl 121.6, KCl 5.4, NaHCO_3 4.013, NaH_2PO_4 0.8, HEPES 10, glucose 5, Na pyruvate 5, MgCl_2 1.8, and CaCl_2 1, pH 7.4. The loaded cells were field-stimulated (5V, 4 milliseconds) at a frequency of 1 Hz. Sarcomere length and fura-2 ratio (measured at 512 nm upon excitation at 340 nm and 380 nm) were simultaneously recorded using an IonOptix System (IonOptix, Westwood, MA). Cell contractility was assessed by the percentage of sarcomere shortening, which is the ratio of twitch amplitude (difference of end-diastolic and peak systolic sarcomere length) to end-diastolic sarcomere length. Ca^{2+} transients were assessed by the percentage of variation of the fura-2 ratio by dividing the twitch amplitude to end-diastolic ratio. The time constant (τ) obtained from the exponential fit of the Ca^{2+} transient decay kinetics was used as an index of relaxation. All parameters were calculated offline using a dedicated software (IonWizard 6x, Westwood, MA).

Western Blot Assay

Protein extracts were prepared from frozen cardiac tissue that were homogenized using a Precellys Evolution Touch Homogenizer (Bertin Technologie) during 3 cycles of 10 seconds at 6500 rpm in a RIPA buffer containing Tris HCl (pH 8.0) 50 mmol/L, NaCl 150 mmol/L, EDTA 2 mmol/L, NP40 1%, sodium deoxycholate acid 0.5%, and SDS 0.1% supplemented with Complete Protease Inhibitor Tablets and PhosSTOP phosphatase inhibitor tablets (Roche Diagnostics, Basel, Switzerland). Tissue lysates were centrifuged at 15000g and 4 °C for 20 minutes, pellets were discarded, and supernatants were used. Protein quantification was performed using a BCA protein assay (Thermo Scientific Pierce, #A55865). 20 μg

of proteins diluted in lithium dodecyl sulfate (Invitrogen, #NP0008) with Sample Reducing Agent (Invitrogen #NP0009) were heated at 70°C for 10 minutes and separated in denaturing acrylamide gels. Subsequently, dry transfer (iBlot2) was performed on PVDF membranes (Invitrogen, #IB24001) for 7 minutes (20V for 1 minute, 23V for 4 minutes and 25V for 2 minutes). After blocking the membranes with 5% milk buffer for 1 hour, the incubation with primary antibodies was carried out overnight at 4°C. After incubation with the appropriate secondary antibody (goat antimouse HRP [horseradish peroxidase], Invitrogen 31430 or goat antirabbit HRP, Invitrogen 31460, diluted at 1/40000), proteins were visualized by enhanced chemiluminescence and quantified with ImageJ software. The primary antibodies used were as follows: (1) **Figure 1**: rabbit anti-PDE2A, Fabgennix; PDE2A-101AP diluted at 1/1000; rabbit anti-GAPDH, Cell Signaling, 2118 diluted at 1/1000; (2) **Figure 2**: goat anti-PDE2A, Santa Cruz, SC-17228 diluted at 1/1000; mouse anti-vinculin, V9131 Sigma-Aldrich diluted at 1/1000; (3) **Figure 3**: rabbit anti-PDE2A, Fabgennix, PDE2A-101AP diluted at 1/1000; rabbit anti-GAPDH, Cell Signaling, 2118 diluted at 1/1000; (4) **Figure S1**: rabbit anti-flag L5, Novus Biologicals, NBP1-06712 diluted at 1/500; rabbit anti-GAPDH, Cell Signaling, 2118 diluted at 1/1000; rabbit anti-PDE2A, Proteintech, 55306-1-AP diluted at 1/1000; rabbit anti-flag L5, Novus Biologicals, NBP1-06712 diluted at 1/500; rabbit anti-GAPDH, Cell Signaling, 2118 diluted at 1/1000; (5) **Figure S2B**: rabbit anti-PDE2A, Proteintech, 55306-1-AP diluted at 1/1000; (6) **Figure S3**: rabbit anti-PDE2A, Proteintech, 55306-1-AP diluted at 1/1000; and (7) **Figure S4**: rabbit anti-PDE4A AC55 (gift from Dr. Marco Conti, University of California San Francisco, San Francisco, CA) diluted at 1/1000; rabbit anti-PDE4B (gift from Dr. Marco Conti) diluted at 1/10000; mouse anti-PDE4D (gift from Dr Marco Conti) diluted at 1/1000 and rabbit anti-PDE3A (gift from Dr Chen Yan, University of Rochester, Rochester, NY) diluted at 1/10000.

Quantitative Real-Time Polymerase Chain Reaction Assay

Using Trizol reagent (MRCgene, Cincinnati, OH), total RNA was extracted from ventricular tissue. Reverse transcription of RNA samples was carried out using iScript cDNA synthesis kit (Bio-Rad, Hercules, CA) according to manufacturer's instructions. Real-time polymerase chain reaction reactions were prepared using SYBR Green Supermix (Bio-Rad, Hercules, CA) and performed in a CFX96 Touch™ Real-Time PCR Detection System (Bio-Rad, Hercules, CA). The relative amount of mRNA transcripts was quantified using the ΔC_t method. *Rplp2* and *Rpl32* housekeeping genes were used as reference for normalization. Sequences of the forward and reverse primers used for each studied gene are given in the 5'-3' orientation:

Pde2a (Forward) TGGGGAAGCTCTTTGACTTGG, (Reverse) ATGACCTTGCAGGAAAGCTG.

Rplp2 (Forward) GCT GTG GCT GTT TCT GCT TC, (Reverse) ATG TCG TCA TCC GAC TCC TCR
Rpl32 (Forward) GCT GCT GAT GTG CAA CAA A, (Reverse) GGG ATT GGT GAC TCT GAT GG.

Additional methods can be found in [Data S1](#).

Statistical Analysis

All results are expressed as mean±SEM and were analyzed using the GraphPad Prism and the R studio software. Normal distribution was tested by D'Agostino and Pearson omnibus normality or Shapiro–Wilk normality tests and homogeneity of variance assessed with the Bartlett's and Levene's tests. When normal distribution and homoscedasticity of values were satisfied, unpaired Student's *t* test or paired Wilcoxon's tests were used for 1 group comparisons, One-way ANOVA or 2-Way ANOVA (ordinary, repeated measure or mixed effects) followed by a Tukey's post hoc test were used to compare differences between multiple groups. When the data did not follow a normal distribution or in case of inhomogeneity of variances, Welch versions of the *t* test and ANOVA, Mann–Whitney *U* test, Kruskal–Wallis test with Dunn's post hoc tests, or an aligned rank transform procedure 2-way mixed ANOVA nested test (Artool) (<https://cran.r-project.org/web/packages/ARTool/readme/README.html>)²⁹ were performed. A Barnard's exact test was used in the analysis of contingency tables. A *P* value <0.05 was considered statistically significant.

RESULTS

Cardiac PDE2A Overexpression in Healthy C57BL/6 Male Mice Does Not Alter the Size, Shape, and Function of the Heart

Constructs including a CMV promoter to allow satisfactory expression of the PDE2A or of the LUC as an internal control of overexpression were built (**Figure S1A**). The AAV9-PDE2A promotes a cAMP-PDE activity that can be repressed by Bay 60–7550 (100 nM), a specific PDE2 inhibitor, demonstrating that the AAV allows overexpression of PDE2A specifically (**Figure S1B**). Before testing the cardioprotective potential of enhanced cardiac PDE2A activity using engineered AAV9, we evaluated the effect of PDE2A overexpression on cardiac function and morphology in healthy mice. A dose of 10¹² viral particles of AAV9-PDE2A or AAV9-LUC were injected into 8-week-old mice and followed up for 28 days (**Figure 1A**). This dose of 10¹² viral particles injected per animal was chosen because the dose–response curve demonstrated that it was required to obtain a firefly activity within the myocardium following

AAV9-LUC injection (Figure S2A). At this dose, the AAV9-PDE2A allows satisfactory expression of PDE2A in the cardiac tissue that, along with the liver, is substantially transduced when the virus is injected into the tail vein. Peripheral expression is limited, with PDE2A slightly expressed in skeletal muscle but not in the kidney (Figure S2B) confirming the preferential cardiac tropism of AAV9, a vector of choice for cardiac gene transfer in rodents.³⁰ As expected, cardiac PDE2A expression was significantly increased in AAV9-PDE2A mice with a ≈ 10 -fold rise of PDE2A protein levels compared with AAV9-LUC mice measured by western blotting (Figure 1B). This overexpression neither affected the heart weight over TL ratio nor the lung weight over TL (Figure 1C). Thus, increasing PDE2A activity in the heart did not provoke cardiac hypertrophy or lung congestion. LV morphology and function evaluated by transthoracic echocardiography remained unaffected by PDE2A with comparable LV weight over body weight ratio. Importantly, ejection fraction measured at 14 and 28 days remained identical in animals receiving AAV9-LUC and AAV9-PDE2A injections (Figure 1D and Table S1). Furthermore, heart rate measured in anesthetized mice as well as other morphological and echocardiographic parameters were not modified by PDE2A overexpression (Table S1).

Cardiac Gene Therapy With PDE2A Limits Left Ventricle Maladaptive Remodeling and Dysfunction Induced by a Chronic Infusion of Sympathomimetic Amines

Because the neurohormonal alterations of HF are characterized by marked elevations in norepinephrine and epinephrine circulating concentrations,³¹ we hypothesized that PDE2A overexpression could exert cardioprotective effects in 2 different mouse models of cardiac dysfunction evoked by chronic infusion with sympathomimetic amines. In both trials, tail vein injections with 10^{12} viral particles of AAV9-LUC or AAV9-PDE2A were performed 14 days before minipump implantation. We first surmised that increased PDE2A activity may mitigate LV remodeling and dysfunction in response to a chronic β -AR stimulation. Thus, we chose to subject the mice to a 14-day infusion with the nonselective β -AR agonist isoproterenol (60 mg/Kg per day).^{15,32} Cardiac function was evaluated in vivo by transthoracic echocardiography over 6 weeks (Figure 2A). Analysis of PDE2A mRNA levels (Figure S5) and protein expression revealed a ≈ 6 -fold increase in the harvested hearts from mice injected with AAV9-PDE2A (Figure 2B). Both groups of mice expressing either LUC or PDE2A implanted with isoproterenol minipumps displayed a similar increase in HR at 2 weeks, attesting the adequate infusion of isoproterenol (Figure S6A).

This treatment resulted in a marked increase of heart weight/TL ratio indicating cardiac hypertrophy ($P=0.0002$), accompanied with lung congestion (lung weight/TL, $P=0.028$) (Figure 2C). Echocardiography confirmed LV hypertrophy and revealed a significantly decreased ejection fraction after 2 weeks' infusion with isoproterenol (Figure 2D). This LV hypertrophy was accompanied with increased end systolic diameter evoking contractile dysfunction, and augmented diastolic LV internal diameter suggesting LV dilation (Table S2). Moreover, Masson's trichrome staining revealed a significant increase in fibrosis after the chronic isoproterenol treatment ($P=0.005$; Figure 2E). Although the heart weight/TL ratio and congestion were only slightly ameliorated in mice overexpressing PDE2A (Figure 2C), LV hypertrophy, systolic dysfunction, myocardial fibrosis, and LV dilation induced by isoproterenol were totally prevented (Figure 2 and Table S2).

Because elevated catecholamines in HF activate not only β -AR but also α -adrenoceptors, we added phenylephrine to isoproterenol in the minipumps at 30 mg/kg per day each. Indeed, the infusion of both amines recapitulates the alterations observed in pressure overload-induced experimental HF and in human hypertrophic cardiomyopathy³³ (Figure 3A). In this set of experiments, a ≈ 12 -fold increase of PDE2A expression in the ventricular tissue was achieved with AAV9 (Figure 3B). Chronic infusion with isoproterenol+phenylephrine induced cardiac hypertrophy and lung congestion as attested by a significant increase in heart weight/TL and lung weight/TL ratios ($P<0.0001$; Figure 3C). These effects were not prevented by PDE2A overexpression despite a trend to diminution (Figure 3C). Similarly, echocardiography revealed a trend for less LV hypertrophy and systolic dysfunction induced by β -AR and α -adrenoceptor stimulation in AAV9-PDE2A mice (Figure 3D and Table S3), despite a persistent LV chamber dilation in diastole and systole (Table S3). Although fibrosis was not significantly reduced by PDE2A overexpression, apoptosis assessed by the TUNEL assay was clearly diminished ($P=0.014$; Figure 3E). Also, gene therapy with PDE2A preserved the diastolic function of the treated mice. Indeed, mice treated with isoproterenol+phenylephrine had a clear diminished transmitral blood flow during the left atrial contraction phase as indicated by the significant decrease of the A wave ($P=0.0002$; Table S3) analyzed with pulse wave Doppler, whereas the E wave, thus compliance, was not improved. This suggests that chronic isoproterenol+phenylephrine treatment altered left atrial contractility, explaining the trend to increased E/A ratio (Table S3). These alterations of the diastolic function induced by sympathomimetic amines were prevented by PDE2A gene therapy, which preserved the contractility of the left atrium (Table S3).

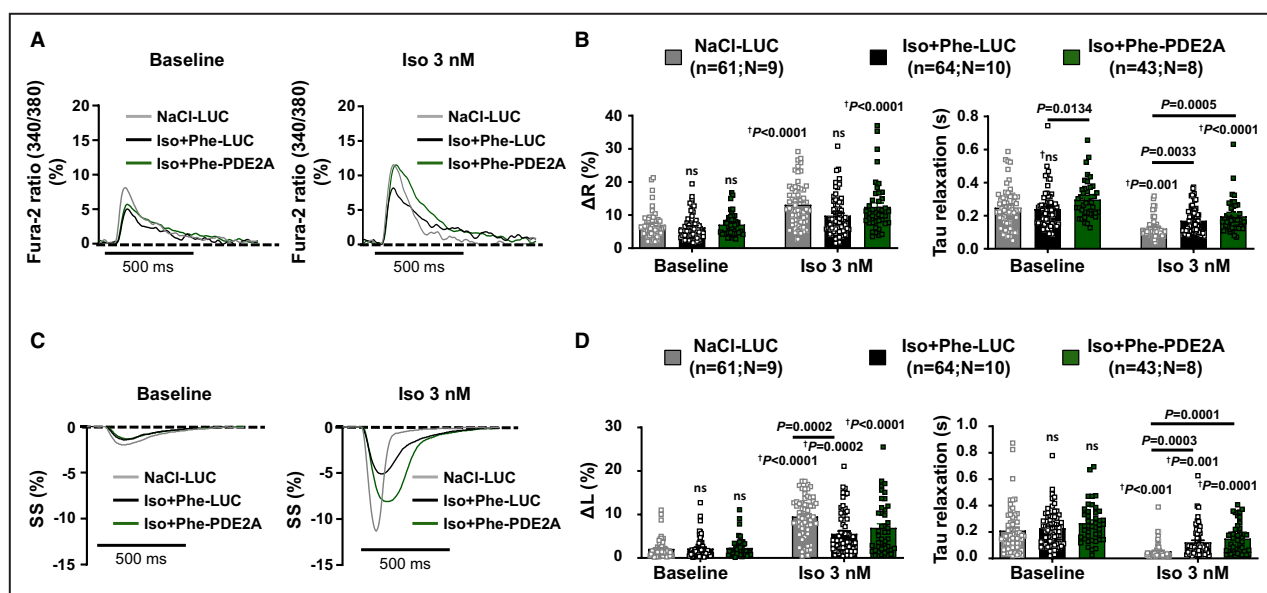


Figure 4. PDE2A overexpression ameliorates the β -AR responsiveness of the excitation-contraction coupling.

A, Representative traces of CaT and **C**, sarcomere shortening obtained simultaneously from ventricular myocytes loaded with fura-2 and paced (1 Hz) isolated from NaCl-LUC (gray), isoproterenol+phenylephrine-LUC (black), or isoproterenol+phenylephrine-PDE2A (green) mice in control conditions and in the presence of 3 nmol/L isoproterenol. **B**, bar graph of mean \pm SEM of the CaT amplitudes (expressed as the percentage of diastolic fura-2 ratio) (left panel) and of the kinetics for return to Ca^{2+} diastolic levels (right panel) in control conditions and in the presence of 3 nmol/L isoproterenol. **D**, bar graph of mean \pm SEM of SS amplitude expressed as the percentage of resting sarcomere length (left panel) and of relaxation time constant (τ , right panel) at baseline and in the presence of 3 nmol/L isoproterenol. SS and CaT were measured in 43 to 64 cells from 9 NaCl-LUC (gray bars), 10 isoproterenol+phenylephrine-LUC (black bars), and 8 isoproterenol+phenylephrine-PDE2A (green bars) mice. Numbers are indicated in the brackets as following (n=number of cells; N=number of mice). Statistical significance indicated by the *P* value (* vs corresponding group at baseline) was determined after an aligned rank transform procedure (ARTool) using a 2-way mixed ANOVA nested test (**B**, **D**). β -AR indicates β -adrenergic receptor; CaT, calcium transients; Iso-Phe-LUC, isoproterenol-phenylephrine-luciferase; Iso-Phe-PDE2A, isoproterenol-phenylephrine-phosphodiesterase 2A; LUC, luciferase; PDE2A, phosphodiesterase 2A; and SS, sarcomere shortening.

PDE2A Improves Defective β -AR Inotropic Effects of Isolated Cardiomyocytes After Chronic Infusion With Sympathomimetic Amines

To investigate how gene therapy with PDE2A affects the ECC and its β -AR modulation at the cellular level, we measured sarcomere shortening (SS) and calcium transients (CaT) simultaneously in fura-2-loaded ventricular myocytes (VMs) paced at 1 Hz. As shown in Figure 4A through 4D, baseline CaT and SS amplitudes and time constants for relaxation (τ) were not modified in VMs from isoproterenol+phenylephrine treated mice although CaT decay was slower in cells overexpressing PDE2A ($P=0.0134$ versus isoproterenol+phenylephrine-LUC, Figure 4B). When challenged with a submaximal concentration of isoproterenol (3 nmol/L), VMs isolated from NaCl-LUC mice had significantly increased CaT and SS amplitudes by 1.9 to 3.5-fold respectively ($P<0.0001$ versus baseline, Figure 4A through 4D and Table S4). Isoproterenol also strongly accelerated the relaxation rates of both CaT and SS ($P=0.001$ versus baseline, Figure 4D). These positive inotropic and lusitropic effects were significantly blunted in VMs isolated from LUC mice

treated with isoproterenol+phenylephrine. Indeed, isoproterenol had no significant effect on CaT amplitude and kinetics whereas SS amplitude increased by only 1.6-fold ($P=0.0002$, versus NaCl-LUC at baseline; Figure 4A through 4D). These blunted effects were not due to increased expression of the main cAMP degrading PDEs expressed in cardiomyocytes because neither PDE2A (Figure S3), PDE3A, PDE4A, PDE4B nor PDE4D protein levels (Figure S4) were significantly affected by chronic isoproterenol+phenylephrine treatment. Interestingly, the positive inotropic effects of isoproterenol were partially restored in VMs from PDE2A-overexpressing animals, although decay times were not improved. Thus, these results demonstrate that gene therapy with PDE2A improves β -AR responsiveness of VMs dampened by chronic infusion with sympathomimetic amines in mice.

PDE2A Cardiac Overexpression Prevents Spontaneous Calcium Events and Ventricular Arrhythmias

It has been previously reported that a constitutive cardiac overexpression of PDE2A had antiarrhythmic effects.^{19,34} We thus tested whether similar effects could

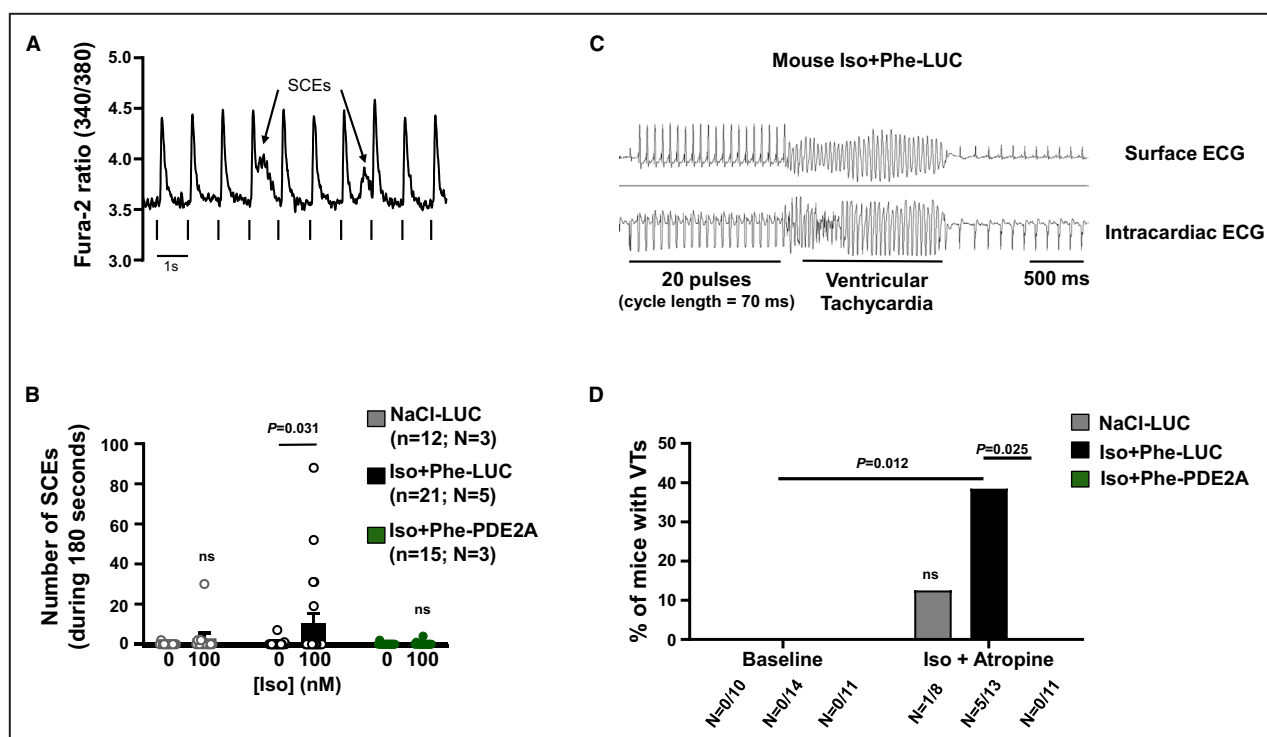


Figure 5. Gene therapy with PDE2A exerts antiarrhythmic effects at the cellular level and in vivo.

A, Representative traces of spontaneous calcium release events pointed by arrow, expressed as the percentage of diastolic fura-2 ratio in paced (1 Hz) ventricular myocytes isolated from isoproterenol+phenylephrine-LUC mice in the presence of 100 nmol/L isoproterenol. **B**, SCEs were counted during the 3 minutes following isoproterenol 100 nmol/L administration. SCEs were measured in 12 to 21 cells isolated from 3 NaCl-LUC (gray), 5 isoproterenol+phenylephrine-LUC (black), and 3 isoproterenol+phenylephrine-PDE2A (green) mice. Numbers are indicated in the brackets as following (n=number of cells; N=number of mice). **C**, Representative examples of simultaneous lead 1 ECG and intraventricular electrogram recordings obtained in a mouse subjected to gene therapy with AAV9-LUC and chronically infused with isoproterenol and phenylephrine (30 mg/kg per day each) for 14 days after paced extrasystoles. The protocol consisted of 20 pulses at a cycle length of 70 milliseconds followed by 1 then 2 then 3 closer pulses (cycle length determined by the refractory period). Ventricular tachycardia was defined as the occurrence after the last paced beat of at least 4 consecutive QRS complexes with a different morphology from that seen in normal sinus rhythm. **D**, Histogram showing the percentage of mice with arrhythmias in all 3 groups (NaCl-LUC, isoproterenol+phenylephrine-LUC, isoproterenol+phenylephrine-PDE2A) at baseline and after isoproterenol 1.5 mg/kg+atropine 1 mg/kg injection. The number of animals presenting VTs per group is indicated beneath the histogram. Statistical significance is indicated by the *P* value (* vs corresponding group at baseline, * isoproterenol+phenylephrine-LUC vs isoproterenol+phenylephrine-PDE2A) determined using Wilcoxon's test (**B**); Barnard's exact test (**D**). AAV9 indicates serotype 9 adeno-associated viruses; Iso-Phe-LUC, isoproterenol-phenylephrine-luciferase; Iso-Phe-PDE2A, isoproterenol-phenylephrine-phosphodiesterase 2A; LUC, luciferase; PDE2A, phosphodiesterase 2A; SCE, spontaneous calcium event; and VT, ventricular tachycardia.

be produced by an overexpression induced from a definite time at adulthood.

First, we investigated the occurrence of proarrhythmic spontaneous calcium events recorded in VMs isolated from the 3 groups of mice stimulated with a maximal isoproterenol concentration of 100 nmol/L (Figure 5A). The time to first spontaneous calcium event and the percentage of cells presenting spontaneous calcium events in each group were similar (Figure S7). However, the number of spontaneous calcium events recorded during a 3-minute period of maximal β -AR stimulation was increased by isoproterenol 100 nM in the isoproterenol+phenylephrine-LUC group, but these cellular proarrhythmic events were nearly absent in cells isolated from the isoproterenol+phenylephrine-PDE2A group (Figure 5B).

Next, we tested the putative antiarrhythmic effect of PDE2A gene therapy *in vivo*. We evaluated the propensity of the treated animals to develop ventricular tachycardia. To do so, intracardiac recordings and pacing were performed. Six-lead ECGs recorded in baseline conditions revealed similar PR interval, QRS complex, and QTc interval durations in NaCl-LUC, isoproterenol+phenylephrine-LUC, and isoproterenol+phenylephrine-PDE2A animals (Table S5). However, isoproterenol+phenylephrine-LUC mice had a significantly lower RR interval ($P=0.0098$ versus NaCl), thus higher heart rate ($P=0.0098$ versus NaCl). Interestingly, despite their similar treatment with sympathomimetic amines, mice injected beforehand with AAV9-PDE2A had a cardiac frequency equivalent to that of control animals (Table S5). Mice were then subjected to catheter-mediated ventricular pacing in baseline

conditions, which did not evoke cardiac arrhythmias in any animal of the 3 groups. Intraperitoneal injections of isoproterenol+atropine (1.5 mg/kg and 1 mg/kg, respectively) were therefore performed to favor ventricular tachycardia occurrence. As expected, in the 3 groups of animals, injection of isoproterenol+atropine significantly increased heart rate, decreased RR and PR intervals, and increased QRS complex durations (but not significantly in NaCl-LUC mice), whereas QTc duration remained stable (Table S5). Although LUC mice treated or not with sympathomimetic amines and animals overexpressing PDE2A had similar ECG parameters following the isoproterenol+atropine injection, they responded differently to ventricular pacing. Indeed, extrastimuli delivered following trains of 20 pulses triggered arrhythmias in only 1 out of 8 NaCl-LUC mice but ventricular tachycardia episodes as depicted in Figure 5C were evoked in 5 out of 13 LUC animals chronically infused with sympathomimetic amines ($P=0.012$ versus baseline). However, none of the 11 mice overexpressing PDE2A had arrhythmias when applying stimuli in a programmed electrical stimulation protocol (Figure 5D). This demonstrates that gene therapy with PDE2A protects from ventricular arrhythmias upon stress conditions. To test whether these antiarrhythmic effects are specific to PDE2A overexpression, we evaluated the potency of PDE4B3 to achieve such protective effects, because we previously reported that gene therapy with this enzyme prevents adverse remodeling in HF mice models.¹⁵ Interestingly, a similar treatment with an AAV9 encoding for PDE4B3 did not produce similar antiarrhythmic effects despite diminished LV hypertrophy and dysfunction (Figures S8A through S8C, Table S6). This demonstrates that protection against ventricular tachycardias evoked by sympathomimetic amines is better achieved with an increase of PDE2A activity than PDE4B3 in this model.

DISCUSSION

Clinically, PDE inhibition has been considered a promising approach to compensate for the β -AR desensitization that accompanies HF. In that respect, PDE3 inhibitors, such as milrinone or enoximone, have been used clinically to improve systolic function and alleviate the symptoms of acute HF. However, their chronic use has proven to be detrimental, increasing adverse remodeling³⁵ and ventricular arrhythmias.^{36,37} These adverse effects could potentially be avoided using compartment-specific, PDE isozyme-selective inhibitors.¹⁰ Here, we proposed to test the opposite strategy, increasing rather than inhibiting PDE activity. We believe that this strategy, which is reminiscent of the counterintuitive beneficial effect of beta blockers in HF, could be therapeutically relevant in HF because it would prevent a deleterious accumulation of cAMP during catecholamine spillover. In that line, we

recently demonstrated that constitutive overexpression of PDE4B,¹⁵ one of the main PDE4 isoforms expressed in the cardiomyocyte to control the β -AR regulation of the ECC,³⁸ is cardioprotective. We also showed that gene therapy with AAV9-PDE4B exerts cardioprotective effects limiting adverse remodeling evoked by isoproterenol or increased postcharge.¹⁵ Similarly, PDE2A constitutive overexpression exerts antihypertrophic effects¹⁸ and transgenic mice overexpressing PDE2A have preserved ejection fraction after myocardial infarction and are protected against sympathomimetic amine-induced ventricular arrhythmia.¹⁹ It was thus important to test whether an increase in PDE2A activity, as obtained during AAV9 gene transfer, could be cardioprotective. Our results are in accordance with a recent study demonstrating that a similar approach not only with PDE4B but also with PDE2A can prevent pressure-overload-induced HF in mice,³⁹ but we further demonstrate with the present study that PDE2A overexpression is more efficient than PDE4B to prevent polymorphic ventricular tachycardia *in vivo*.

Similarly to what we reported earlier in the transgenic mice,¹⁹ here we found that overexpression of PDE2A obtained after systemic injection of the AAV9 construct did not produce any noticeable change either on the left ventricle size or on its function. Morphometric parameters were not affected by the overexpression of PDE2A, and contractile parameters were preserved with no congestion.

The safety of this treatment allowed us to move forward and test whether overexpression of PDE2A would counteract the adverse remodeling evoked by catecholamines. Indeed, AAV9 delivery of PDE2A efficiently protected against the detrimental effects of chronic isoproterenol treatment. Chronic sympathomimetic amine infusion models promote cardiomyocyte death and contractile cells are then replaced by interstitial fibrosis.⁴⁰ AAV9-mediated PDE2A overexpression counteracted the systolic dysfunction, attenuated the hypertrophic response, and efficiently prevented fibrosis, a hallmark of pathological remodeling. These cardioprotective effects against β -AR chronic stimulation were as effective as the one obtained by gene therapy with PDE4B,¹⁵ confirming that increasing PDE activity is effective to counteract adverse remodeling evoked by catecholamines. However, elevated catecholamines act not only via β -AR but also via α -adrenoceptors. Interestingly, gene therapy with PDE2A (and PDE4B, Figure S8) was able to limit LV hypertrophy and dysfunction induced by isoproterenol+phenylephrine challenge, a situation that recapitulates more effectively early transcriptional alterations observed in pressure overload-induced experimental HF and in human hypertrophic cardiomyopathy.³³ Cardioprotective effects of PDE2A overexpression were less pronounced with isoproterenol+phenylephrine than with isoproterenol alone, probably because PDE2A is less efficient

in counteracting cAMP-independent effects of α_1 -AR stimulation such as apoptosis and fibrosis³³ than cAMP-signaling emanating from β -AR stimulation. Nevertheless, adverse remodeling and LV dysfunction were reduced by PDE2A overexpression.

Our results demonstrate that gene therapy with PDE2A improves cardiac adaptation to catecholaminergic stress. Indeed, we found that PDE2A cardiac overexpression led to a better responsiveness of the ECC to the β -AR agonist, which could be explained by decreased intracellular cAMP levels upon chronic β -AR activation known to promote heterologous desensitization of the receptors by promoting their phosphorylation by PKA.⁴¹ Interestingly, a similar receptor “resensitization” evoked by gene therapy with PDE2A of the β_1 -AR/cAMP production was recently reported in ventricular cardiomyocytes isolated from mice in HF induced by increased postcharge.³⁹ This may contribute to the improved ejection fraction we observed in animals subjected to gene therapy with PDE2A. However, overexpression of PDE2A failed to improve the lusitropic effects of isoproterenol in cardiomyocytes. This is likely because, as shown earlier, PDE2 is enriched in the vicinity of the sarco/endoplasmic reticulum Ca^{2+} -ATPase, especially under pathological conditions,⁴² and PDE2 gene therapy further increases the activity of the enzyme in this compartment,³⁹ leading to a slower CaT decay upon isoproterenol as observed (Figure 4B). This could explain why compliance of the left ventricle, estimated by the E wave in echocardiography, was not improved by PDE2A. Nonetheless, diastolic dysfunction evoked by the chronic amines treatment was less pronounced when PDE2A was overexpressed, due to ameliorated atrial contractility estimated by the A wave (Table S3). Prolonged CaT due to decreased SERCA2 (sarco/endoplasmic reticulum Ca^{2+} ATPase) activity by PDE2A suggests that this treatment could increase diastolic Ca^{2+} levels and thus, promote arrhythmias. In contrast, myocytes isolated from animals treated with PDE2 gene therapy exhibited fewer spontaneous proarrhythmogenic calcium events upon β -AR stimulation. This is in agreement with what was observed in cells isolated from hearts overexpressing PDE2A, probably by preventing the Epac- and CaMKII-mediated increase of the late sodium current (I_{NaL}) and Ca^{2+} leakage via RyR2 as recently described in cardiomyocytes from PDE2A transgenic mice.³⁴ Furthermore, it was recently demonstrated that gene therapy with PDE2A in HF induced by increased postcharge could restore partially cAMP compartmentation at the vicinity of the RyR2.³⁹ These phenomena could also contribute to improve the cardiac function and decrease the propensity of these animals to trigger ventricular arrhythmias as we unveil here, in accordance with the protection conferred by PDE2A constitutive overexpression in the setting of myocardial infarction previously described.¹⁹

Although we showed that PDE2A overexpression is cardioprotective,¹⁸ another group showed that inhibition rather than increased activity of PDE2 exerts positive outcome in a pressure-overload model.²⁵ Furthermore, under pathologic conditions PDE2A overexpression was proposed to increase ventricular cardiomyocyte size, thus to evoke adverse remodeling.²² Although it was demonstrated that PDE2 regulates cGMP generated by particulate guanylate cyclases,⁴³ the cardioprotective effects of PDE2 inhibition were attributed to increased cGMP emanating from the nitrous oxide stimulated soluble guanylyl cyclase.²⁵ However, PDE2 inhibition by promoting voltage-gated Ca^{2+} transients in postganglionic neurons from stellate ganglia increases cardiac neurotransmission,⁴⁴ a mechanism that may also contribute to increase cardiac function and alleviate cardiac dysfunction. Moreover, global PDE2 inhibition induced a modest coronary vasodilatation,²⁵ which could have contributed to the beneficial effects observed.

Here, using AAV9, which has the highest expression in the heart among AAV serotypes,²⁶ we believe that the observed cardioprotective effects are achieved due to a preferential cardiac overexpression of PDE2. Interestingly, activating mutations in another PDE, PDE3, responsible for a rare disease characterized by the combination of brachydactyly and hypertension, confers cardioprotection despite the increase in afterload.⁴⁵ The latter observation supports our initial postulate and our observations reported here and earlier¹⁵ that increasing rather than decreasing the activity of PDEs in cardiac tissue is beneficial. However, it remains to be demonstrated which PDE will be the most effective to achieve this goal. We show here that gene therapy with PDE2A is as effective as PDE4B in counteracting the adverse remodeling of the left ventricle and systolic dysfunction induced by chronic catecholamines infusion but more efficient in counteracting stress-induced ventricular tachycardia. This difference may come from the intrinsic characteristics of the 2 enzymes. Indeed, PDE2A has a 20-fold lower affinity for cAMP than PDE4B ($K_m=30$ versus $1.5\text{--}4.7\text{ }\mu\text{mol/L}$), and a ~ 1000 -fold higher hydrolytic activity ($V_{\text{max}}=120$ versus $0.13\text{ }\mu\text{mol/min per mg protein}$).⁴⁶ Thus, PDE2A would be turned on only when cAMP concentration reaches supraphysiological values, and its high V_{max} would tend to rapidly reduce it to normal. In other words, PDE2A might serve as a safety valve to avoid the cell being flooded with cAMP. In contrast, PDE4B degrades cAMP at physiological concentrations and, as such, plays a more essential role in the regulation of ECC.³⁸ Its overexpression will thus have different consequences on heart function, notably by reducing the β -AR response of the heart. Of note, and on the contrary to PDE4B, PDE2A is a cGMP-activated PDE⁴⁷ and its cAMP-hydrolytic activity can be increased ~ 30 fold upon cGMP binding to its GAFB domain. cGMP

elevation, which has been shown to be cardioprotective in HF,⁴⁸ could be achieved by activating the particulate guanylyl cyclase localized near PDE2A,⁴³ to constitute a NP (natriuretic peptide)/BNP (B-type natriuretic peptide)/cGMP-triggered defense mechanism during cardiac stress, in particular during excessive β -AR drive. Interestingly, sacubitril, which further elevates NPs, improves classical treatments for HF,⁴⁹ and it has been recently demonstrated that NPs exert antiarrhythmic effects via PDE2.²³

LIMITATIONS

There are 3 main limitations to our study. First, only male mice were used here. Sex-dependent heterogeneity in β -AR/cAMP signaling has been shown recently,^{50–52} which may have substantial functional implications in both normal and diseased hearts. Therefore, future experiments should be performed in female mice to examine possible differences in the cardioprotective effect of PDE2A gene therapy between male and female animals. Second, we used here 2 models of hypertrophy and dysfunction induced by chronic infusion of either isoproterenol or isoproterenol + phenylephrine, a situation that recapitulates early transcriptional alterations observed in pressure overload-induced experimental HF and in human hypertrophic cardiomyopathy.³³ However, because PDEs are part of the signaling pathway downstream of the catecholamine stress, PDE2A overexpression may have interfered with the effectiveness of catecholamines to injure the heart. Although this might be one reason for the efficacy of PDE2A gene therapy, other experimental models to induce HF should be tested in the future, such as myocardial infarction or transverse aortic constriction. Finally, it would be important to investigate what happens if the PDE2 gene therapy is applied after the myocardial dysfunction has taken place to explore the potential curative effect of the treatment.

CONCLUSIONS

Our results demonstrate that increasing PDE2A activity is beneficial in HF. They suggest that a gene therapy with PDE2A in cardiac cells, or PDE2A activators yet to be discovered, could be of therapeutic value. We can therefore speculate that further beneficial effects could be obtained with a gene therapy with PDE2, which could constitute a complement to neprilysin inhibitors and actual treatments of chronic HF to limit adverse remodeling and accompanying arrhythmias.

ARTICLE INFORMATION

Received August 19, 2024; accepted December 23, 2024.

Affiliations

Université Paris-Saclay, Inserm, Signaling and Cardiovascular Pathophysiology, UMR-S 1180, Orsay, France (R.K., A.B., J.P.M., V.J., A.V., D.M., V.A., R.F., G.V., J.L.); Molecular Biotechnology Center “Guido Tarone”, Department of Molecular Biotechnology and Health Sciences, University of Torino, Italy (J.P.M., A.G., E.H.); Nantes Université, CNRS, INSERM, l’Institut du thorax, Nantes, France (A.H., F.C.); Université Paris-Saclay, Inserm US31, CNRS UMS3679, IPSIT, Orsay, France (F.M.); and Cystic Kidney Disorders Unit, Division of Genetics and Cell Biology, Università Vita-Salute San Raffaele, Milan, Italy (J.P.M.).

Acknowledgments

Author contributions: Jérôme Leroy, Alessandra Ghigo, Flavien Charpentier, Emilio Hirsch, Rodolphe Fischmeister, Grégoire Vandecasteele contributed to conception and experimental design. Rima Kamel, Aurélia Bourcier, and Jean Piero Margaria performed osmotic pump implantation and echocardiography studies. Aurélia Bourcier, Agnès Hivonnait, Flavien Charpentier, and Vincent Algalarrondo, and Audrey Varin performed and analyzed in vivo ECG recording and intracardiac recording and pacing experiments. Jean Piero Margaria, Aurélia Bourcier, and Audrey Varin performed real-time quantitative polymerase chain reaction and Western blot experiments. Delphine Mika and Jean Piero Margaria performed the PDE assays. Rima Kamel was in charge of cell isolation and performed and analyzed single cell Ca^{2+} transients and contractility experiments. Françoise Mercier-Nomé was in charge of the morphological and histological analysis. Rima Kamel, Aurélia Bourcier, and Jean Piero Margaria prepared the figures and wrote the first draft of the article. All authors contributed to editing the final version of the article.

Sources of Funding

UMR-S1180 is a member of the Laboratory of Excellence LERMIT supported by the French National Research Agency (ANR-10-LABX-33) under the program “Investissements d’Avenir” ANR-11-IDEX-0003-01. This work was also funded by grants from the Leducq Foundation for Cardiovascular Research (19CVD02), ERA-CVD “PDE4HEART”, ANR-16-ECVD-0007-01, and EU MILEAGE project #734931 to Rodolphe Fischmeister; the DIM BioConvS of Région Ile-de-France 2023 equip-IL-536836, ANR-19-CE14-0038-02 and ANR-21-CE14-0082-01 to Grégoire Vandecasteele; ANR-23-CE14-0051-01 to Jérôme Leroy; and Fédération Française de Cardiologie to Vincent Algalarrondo. Rima Kamel was supported by postdoctoral fellowships from ERA-CVD and Fondation Lefoulon-Delalande. For the purpose of open access, the authors have applied a CC-BY public copyright license to any Author Accepted Manuscript version arising from this submission.

Disclosures

Alessandra Ghigo and Emilio Hirsch are cofounders and shareholders of Kither Biotech, a pharmaceutical product company developing PI3K inhibitors for the treatment of respiratory diseases not in conflict with statements made in this article. The remaining authors have no disclosures to report.

Supplemental Material

Data S1
Tables S1–S6
Figures S1–S8
Reference 53

REFERENCES

1. Papa A, Kushner J, Marx SO. Adrenergic regulation of calcium channels in the heart. *Annu Rev Physiol*. 2022;84:285–306. doi: [10.1146/annurev-physiol-060121-041653](https://doi.org/10.1146/annurev-physiol-060121-041653)
2. Liu G, Papa A, Katchman AN, Zakharov SI, Roybal D, Hennessey JA, Kushner J, Yang L, Chen BX, Kushnir A, et al. Mechanism of adrenergic CaV1.2 stimulation revealed by proximity proteomics. *Nature*. 2020;577:695–700. doi: [10.1038/s41586-020-1947-z](https://doi.org/10.1038/s41586-020-1947-z)
3. Cohn JN, Levine TB, Olivari MT, Garberg V, Lura D, Francis GS, Simon AB, Rector T. Plasma norepinephrine as a guide to prognosis in patients with chronic congestive heart failure. *N Engl J Med*. 1984;311:819–823. doi: [10.1056/NEJM198409273111303](https://doi.org/10.1056/NEJM198409273111303)
4. Ponikowski P, Voors AA, Anker SD, Bueno H, Cleland JGF, Coats AJS, Falk V, Gonzalez-Juanatey JR, Harjola VP, Jankowska EA, et al. 2016 ESC guidelines for the diagnosis and treatment of acute and chronic

- heart failure: the task force for the diagnosis and treatment of acute and chronic heart failure of the European Society of Cardiology (ESC) developed with the special contribution of the Heart Failure Association (HFA) of the ESC. *Eur Heart J*. 2016;37:2129–2200. doi: [10.1093/eurheartj/ehw128](https://doi.org/10.1093/eurheartj/ehw128)
5. Packer M, Bristow MR, Cohn JN, Colucci WS, Fowler MB, Gilbert EM, Shusterman NH. The effect of carvedilol on morbidity and mortality in patients with chronic heart failure. U.S. Carvedilol Heart Failure Study Group. *N Engl J Med*. 1996;334:1349–1355. doi: [10.1056/NEJM199605233342101](https://doi.org/10.1056/NEJM199605233342101)
 6. Ziaeian B, Fonarow GC. Epidemiology and aetiology of heart failure. *Nat Rev Cardiol*. 2016;13:368–378. doi: [10.1038/nrcardio.2016.25](https://doi.org/10.1038/nrcardio.2016.25)
 7. Investigators M-H. Effect of metoprolol CR/XL in chronic heart failure: Metoprolol CR/XL Randomised Intervention Trial in Congestive Heart Failure (MERIT-HF). *Lancet*. 1999;353:2001–2007. doi: [10.1016/S0140-6736\(99\)04440-2](https://doi.org/10.1016/S0140-6736(99)04440-2)
 8. Levy D, Kenchaiah S, Larson MG, Benjamin EJ, Kupka MJ, Ho KK, Murabito JM, Vasan RS. Long-term trends in the incidence of and survival with heart failure. *N Engl J Med*. 2002;347:1397–1402. doi: [10.1056/NEJMoa020265](https://doi.org/10.1056/NEJMoa020265)
 9. Bhatt AS, DeVore AD, DeWald TA, Swedberg K, Mentz RJ. Achieving a maximally tolerated β -blocker dose in heart failure patients: is there room for improvement? *J Am Coll Cardiol*. 2017;69:2542–2550. doi: [10.1016/j.jacc.2017.03.563](https://doi.org/10.1016/j.jacc.2017.03.563)
 10. Kamel R, Leroy J, Vandecasteele G, Fischmeister R. Phosphodiesterases as therapeutic targets in cardiac hypertrophy and heart failure. *Nat Rev Cardiol*. 2023;20:90–108. doi: [10.1038/s41569-022-00756-z](https://doi.org/10.1038/s41569-022-00756-z)
 11. Rivet-Bastide M, Vandecasteele G, Hatem S, Verde I, Benardeau A, Mercadier JJ, Fischmeister R. cGMP-stimulated cyclic nucleotide phosphodiesterase regulates the basal calcium current in human atrial myocytes. *J Clin Invest*. 1997;99:2710–2718. doi: [10.1172/JCI119460](https://doi.org/10.1172/JCI119460)
 12. Wang YW, Gao QW, Xiao YJ, Zhu XJ, Gao L, Zhang WH, Wang RR, Chen KS, Liu FM, Huang HL, et al. Bay 60-7550, a PDE2 inhibitor, exerts positive inotropic effect of rat heart by increasing PKA-mediated phosphorylation of phospholamban. *Eur J Pharmacol*. 2021;901:174077. doi: [10.1016/j.ejphar.2021.174077](https://doi.org/10.1016/j.ejphar.2021.174077)
 13. Mika D, Bobin P, Pomérance M, Lechène P, Westenbroek R, Catterall WA, Vandecasteele G, Leroy J, Fischmeister R. Differential regulation of cardiac excitation-contraction coupling by cAMP phosphodiesterase subtypes. *Cardiovasc Res*. 2013;100:336–346. doi: [10.1093/cvr/cvt193](https://doi.org/10.1093/cvr/cvt193)
 14. Mongillo M, Tocchetti CG, Terrin A, Lissandron V, Cheung YF, Dostmann WR, Pozzan T, Kass DA, Paolocci N, Houslay MD, et al. Compartmentalized phosphodiesterase-2 activity blunts β -adrenergic cardiac inotropy via an NO/cGMP-dependent pathway. *Circ Res*. 2006;98:226–234. doi: [10.1161/01.RES.0000200178.34179.93](https://doi.org/10.1161/01.RES.0000200178.34179.93)
 15. Karam S, Margaria JP, Bourcier A, Mika D, Varin A, Bedioun I, Lindner M, Bouadjel K, Dessillons M, Gaudin F, et al. Cardiac overexpression of PDE4B blunts β -adrenergic response and maladaptive remodeling in heart failure. *Circulation*. 2020;142:161–174. doi: [10.1161/CIRCULATIONAHA.119.042573](https://doi.org/10.1161/CIRCULATIONAHA.119.042573)
 16. Mika D, Bobin P, Lindner M, Boet A, Hodzic A, Lefebvre F, Lechène P, Sadoune M, Samuel JL, Algallarrondo V, et al. Synergic PDE3 and PDE4 control intracellular cAMP and cardiac excitation-contraction coupling in a porcine model. *J Mol Cell Cardiol*. 2019;133:57–66. doi: [10.1016/j.yjmcc.2019.05.025](https://doi.org/10.1016/j.yjmcc.2019.05.025)
 17. Abi-Gerges A, Richter W, Lefebvre F, Matéo P, Varin A, Heymes C, Samuel J-L, Lugnier C, Conti M, Fischmeister R, et al. Decreased expression and activity of cAMP phosphodiesterases in cardiac hypertrophy and its impact on β -adrenergic cAMP signals. *Circ Res*. 2009;105:784–792. doi: [10.1161/CIRCRESAHA.109.197947](https://doi.org/10.1161/CIRCRESAHA.109.197947)
 18. Mehler H, Emons J, Vettel C, Wittköpper K, Seppelt D, Dewenter M, Lutz S, Sossalla S, Maier LS, Lechène P, et al. Phosphodiesterase-2 is up-regulated in human failing hearts and blunts β -adrenergic responses in cardiomyocytes. *J Am Coll Cardiol*. 2013;62:1596–1606. doi: [10.1016/j.jacc.2013.05.057](https://doi.org/10.1016/j.jacc.2013.05.057)
 19. Vettel C, Lindner M, Dewenter M, Lorenz K, Schanbacher C, Riedel M, Lämmle S, Meinecke S, Mason F, Sossalla S, et al. Phosphodiesterase 2 protects against catecholamine-induced arrhythmias and preserves contractile function after myocardial infarction. *Circ Res*. 2017;120:120–132. doi: [10.1161/CIRCRESAHA.116.310069](https://doi.org/10.1161/CIRCRESAHA.116.310069)
 20. Martinez SE, Wu AY, Glavas NA, Tang XB, Turley S, Hol WG, Beavo JA. The two GAF domains in phosphodiesterase 2A have distinct roles in dimerization and in cGMP binding. *Proc Natl Acad Sci USA*. 2002;99:13260–13265. doi: [10.1073/pnas.192374899](https://doi.org/10.1073/pnas.192374899)
 21. Weber S, Zeller M, Guan K, Wunder F, Wagner M, El-Armouche A. PDE2 at the crossway between cAMP and cGMP signalling in the heart. *Cell Signal*. 2017;38:76–84. doi: [10.1016/j.cellsig.2017.06.020](https://doi.org/10.1016/j.cellsig.2017.06.020)
 22. Zoccarato A, Surdo NC, Aronsen JM, Fields LA, Mancuso L, Dodoni G, Stangherlin A, Livie C, Jiang H, Sin YY, et al. Cardiac hypertrophy is inhibited by a local pool of cAMP regulated by phosphodiesterase 2. *Circ Res*. 2015;117:707–719. doi: [10.1161/CIRCRESAHA.114.305892](https://doi.org/10.1161/CIRCRESAHA.114.305892)
 23. Cachorro E, Gunscht M, Schubert M, Sadek MS, Siegert J, Dutt F, Bauermeister C, Quickert S, Berning H, Nowakowski F, et al. CNP promotes antiarrhythmic effects via phosphodiesterase 2. *Circ Res*. 2023;132:400–414. doi: [10.1161/CIRCRESAHA.122.322031](https://doi.org/10.1161/CIRCRESAHA.122.322031)
 24. Monterisi S, Lobo MJ, Livie C, Castle JC, Weinberger M, Baillie GS, Surdo NC, Musheshe N, Stangherlin A, Gottlieb E, et al. PDE2A2 regulates mitochondria morphology and apoptotic cell death via local modulation of cAMP/PKA signalling. *eLife*. 2017;6:e21374. doi: [10.7554/eLife.21374](https://doi.org/10.7554/eLife.21374)
 25. Baliga RS, Preedy MEJ, Dukinfield MS, Chu SM, Aubdool AA, Bubb KJ, Moyes AJ, Tones MA, Hobbs AJ. Phosphodiesterase 2 inhibition preferentially promotes NO/guanylyl cyclase/cGMP signaling to reverse the development of heart failure. *Proc Natl Acad Sci USA*. 2018;115:E7428–E7437. doi: [10.1073/pnas.1800996115](https://doi.org/10.1073/pnas.1800996115)
 26. Zicarelli C, Soltys S, Rengo G, Rabinowitz JE. Analysis of AAV serotypes 1–9 mediated gene expression and tropism in mice after systemic injection. *Mol Ther*. 2008;16:1073–1080. doi: [10.1038/mt.2008.76](https://doi.org/10.1038/mt.2008.76)
 27. Royer A, van Veen TA, Le Bouter S, Marionneau C, Griol-Charhbil V, Leoni AL, Steenman M, van Rijen HV, Demolombe S, Goddard CA, et al. Mouse model of SCN5A-linked hereditary Lenegre's disease: age-related conduction slowing and myocardial fibrosis. *Circulation*. 2005;111:1738–1746. doi: [10.1161/01.CIR.0000160853.19867.61](https://doi.org/10.1161/01.CIR.0000160853.19867.61)
 28. Mitchell GF, Jeron A, Koren G. Measurement of heart rate and Q-T interval in the conscious mouse. *Am J Phys*. 1998;274:H747–H751. doi: [10.1152/ajpheart.1998.274.3.H747](https://doi.org/10.1152/ajpheart.1998.274.3.H747)
 29. Wobbrock JO, Findlater L, Gergle D, Higgins JJ. The aligned rank transform for nonparametric factorial analyses using only anova procedures. CHI '11: Proceedings of the SIGCHI Conference on Human Factors in Computing Systems. 2011:143–146.
 30. Bish LT, Morine K, Sleeper MM, Sanmiguel J, Wu D, Gao G, Wilson JM, Sweeney HL. Adeno-associated virus (AAV) serotype 9 provides global cardiac gene transfer superior to AAV1, AAV6, AAV7, and AAV8 in the mouse and rat. *Hum Gene Ther*. 2008;19:1359–1368. doi: [10.1089/hum.2008.123](https://doi.org/10.1089/hum.2008.123)
 31. Lympopoulos A, Rengo G, Koch WJ. Adrenergic nervous system in heart failure: pathophysiology and therapy. *Circ Res*. 2013;113:739–753. doi: [10.1161/CIRCRESAHA.113.300308](https://doi.org/10.1161/CIRCRESAHA.113.300308)
 32. Irie T, Sips PY, Kai S, Kida K, Ikeda K, Hirai S, Moazzami K, Jiramongkolchai P, Bloch DB, Doulias PT, et al. S-nitrosylation of calcium-handling proteins in cardiac adrenergic signaling and hypertrophy. *Circ Res*. 2015;117:793–803. doi: [10.1161/CIRCRESAHA.115.307157](https://doi.org/10.1161/CIRCRESAHA.115.307157)
 33. Dewenter M, Pan J, Knodler L, Tzschockel N, Henrich J, Cordero J, Dobrev G, Lutz S, Backs J, Wieland T, et al. Chronic isoprenaline/phenylephrine vs. exclusive isoprenaline stimulation in mice: critical contribution of α 1-adrenoceptors to early cardiac stress responses. *Basic Res Cardiol*. 2022;117:15. doi: [10.1007/s00395-022-00920-z](https://doi.org/10.1007/s00395-022-00920-z)
 34. Wagner M, Sadek MS, Dybkova N, Mason FE, Klehr J, Firneburg R, Cachorro E, Richter K, Klapproth E, Kuenzel SR, et al. Cellular mechanisms of the anti-arrhythmic effect of cardiac PDE2 overexpression. *Int J Mol Sci*. 2021;22:4816. doi: [10.3390/ijms22094816](https://doi.org/10.3390/ijms22094816)
 35. Ding B, Abe J, Wei H, Huang Q, Walsh RA, Molina CA, Zhao A, Sadoshima J, Blaxall BC, Berk BC, et al. Functional role of phosphodiesterase 3 in cardiomyocyte apoptosis: implication in heart failure. *Circulation*. 2005;111:2469–2476. doi: [10.1161/01.CIR.0000165128.39715.87](https://doi.org/10.1161/01.CIR.0000165128.39715.87)
 36. Holmes JR, Kubo SH, Cody RJ, Kligfield P. Milrinone in congestive heart failure: observations on ambulatory ventricular arrhythmias. *Am Heart J*. 1985;110:800–806. doi: [10.1016/0002-8703\(85\)90460-0](https://doi.org/10.1016/0002-8703(85)90460-0)
 37. Packer M, Carver JR, Rodeheffer RJ, Ivanhoe RJ, DiBianco R, Zeldis SM, Hendrix GH, Bommer WJ, Elkayam U, Kukin ML, et al. Effect of oral milrinone on mortality in severe chronic heart failure. The PROMISE study research group. *N Engl J Med*. 1991;325:1468–1475. doi: [10.1056/NEJM199111233251203](https://doi.org/10.1056/NEJM199111233251203)
 38. Leroy J, Richter W, Mika D, Castro LRV, Abi-Gerges A, Xie M, Scheitrum C, Lefebvre F, Schittl J, Westenbroek R, et al. Phosphodiesterase 4B in the cardiac L-type Ca^{2+} channel complex regulates Ca^{2+} current and protects against ventricular arrhythmias. *J Clin Invest*. 2011;121:2651–2661. doi: [10.1172/JCI44747](https://doi.org/10.1172/JCI44747)

39. Pavlaki N, Froese A, Li W, De Jong KA, Geertz B, Subramanian H, Mohagaonkar S, Luo X, Schubert M, Wiegmann R, et al. Gene therapy with phosphodiesterases 2A and 4B ameliorates heart failure and arrhythmias by improving subcellular cAMP compartmentation. *Cardiovasc Res*. 2024;120:1011–1023. doi: [10.1093/cvr/cvae094](https://doi.org/10.1093/cvr/cvae094)
40. Benjamin IJ, Jalil JE, Tan LB, Cho K, Weber KT, Clark WA. Isoproterenol-induced myocardial fibrosis in relation to myocyte necrosis. *Circ Res*. 1989;65:657–670. doi: [10.1161/01.RES.65.3.657](https://doi.org/10.1161/01.RES.65.3.657)
41. Rockman HA, Koch WJ, Lefkowitz RJ. Seven-transmembrane-spanning receptors and heart function. *Nature*. 2002;415:206–212. doi: [10.1038/415206a](https://doi.org/10.1038/415206a)
42. Sprenger JU, Perera RK, Steinbrecher JH, Lehnart SE, Maier LS, Hasenfuss G, Nikolaev VO. In vivo model with targeted cAMP biosensor reveals changes in receptor-microdomain communication in cardiac disease. *Nat Commun*. 2015;6:6965. doi: [10.1038/ncomms7965](https://doi.org/10.1038/ncomms7965)
43. Castro LR, Verde I, Cooper DMF, Fischmeister R. Cyclic guanosine monophosphate compartmentation in rat cardiac myocytes. *Circulation*. 2006;113:2221–2228. doi: [10.1161/CIRCULATIONAHA.105.599241](https://doi.org/10.1161/CIRCULATIONAHA.105.599241)
44. Wang L, Henrich M, Buckler KJ, McMenamin M, Mee CJ, Sattelle DB, Paterson DJ. Neuronal nitric oxide synthase gene transfer decreases $[Ca^{2+}]_i$ in cardiac sympathetic neurons. *J Mol Cell Cardiol*. 2007;43:717–725. doi: [10.1016/j.yjmcc.2007.09.005](https://doi.org/10.1016/j.yjmcc.2007.09.005)
45. Ercu M, Mucke MB, Pallien T, Marko L, Sholokh A, Schachterle C, Aydin A, Kidd A, Walter S, Esmati Y, et al. Mutant phosphodiesterase 3A protects from hypertension-induced cardiac damage. *Circulation*. 2022;146:1758–1778. doi: [10.1161/CIRCULATIONAHA.122.060210](https://doi.org/10.1161/CIRCULATIONAHA.122.060210)
46. Bender AT, Beavo JA. Cyclic nucleotide phosphodiesterases: from molecular regulation to clinical use. *Pharmacol Rev*. 2006;58:488–520. doi: [10.1124/pr.58.3.5](https://doi.org/10.1124/pr.58.3.5)
47. Martins TJ, Mumby MC, Beavo JA. Purification and characterization of a cyclic GMP-stimulated cyclic nucleotide phosphodiesterase from bovine tissues. *J Biol Chem*. 1982;257:1973–1979. doi: [10.1016/S0021-9258\(19\)68134-2](https://doi.org/10.1016/S0021-9258(19)68134-2)
48. Numata G, Takimoto E. Cyclic GMP and PKG signaling in heart failure. *Front Pharmacol*. 2022;13:792798. doi: [10.3389/fphar.2022.792798](https://doi.org/10.3389/fphar.2022.792798)
49. McMurray JJ, Packer M, Desai AS, Gong J, Lefkowitz MP, Rizkala AR, Rouleau JL, Shi VC, Solomon SD, Swedberg K, et al. Angiotensin-neprilysin inhibition versus enalapril in heart failure. *N Engl J Med*. 2014;371:993–1004. doi: [10.1056/NEJMoa1409077](https://doi.org/10.1056/NEJMoa1409077)
50. Prajapati C, Koivumaki J, Pekkanen-Mattila M, Aalto-Setälä K. Sex differences in heart: from basics to clinics. *Eur J Med Res*. 2022;27:241. doi: [10.1186/s40001-022-00880-z](https://doi.org/10.1186/s40001-022-00880-z)
51. Caldwell JL, Lee IJ, Ngo L, Wang L, Bahriz S, Xu B, Bers DM, Navedo MF, Bossuyt J, Xiang YK, et al. Whole-heart multiparametric optical imaging reveals sex-dependent heterogeneity in cAMP signaling and repolarization kinetics. *Sci Adv*. 2023;9:eadd5799. doi: [10.1126/sciadv.add5799](https://doi.org/10.1126/sciadv.add5799)
52. Parks RJ, Ray G, Bienvenu LA, Rose RA, Howlett SE. Sex differences in SR Ca release in murine ventricular myocytes are regulated by the cAMP/PKA pathway. *J Mol Cell Cardiol*. 2014;75:162–173. doi: [10.1016/j.yjmcc.2014.07.006](https://doi.org/10.1016/j.yjmcc.2014.07.006)
53. Thompson WJ, Appleman MM. Multiple cyclic nucleotide phosphodiesterase activities from rat brain. *Biochemistry*. 1971;10:311–316. doi: [10.1021/bi00778a018](https://doi.org/10.1021/bi00778a018)